SUPPLEMENTARY MATERIAL for ID CC-COM-09-2013-047370

A novel, rigid diphosphine with an active NHC spacer; di- and trinuclear complexes of d^{10} coinage metals

Pengfei Ai,[a] Andreas A. Danopoulos,*[a,b] Pierre Braunstein*[a] and Kirill Yu. Monakhov[c]

[a] *Laboratoire de Chimie de Coordination, Institut de Chimie (UMR 7177 CNRS), Université de Strasbourg, 4 rue Blaise Pascal, 67081 Strasbourg Cedex (France). E-mail: danopoulos@unistra.fr, braunstein@unistra.fr*

[b] *Institute for Advanced Study, University of Strasbourg (USIAS)*

[c] *Institut für Anorganische Chemie, RWTH Aachen University, Landoltweg 1, 52074 Aachen, Germany*

Contents:

1. Synthesis and characterisation

1.1 General methods

All manipulations involving organometallics were performed under nitrogen or argon in a Braun glove-box or using standard Schlenk techniques. Solvents were dried using standard methods and distilled under nitrogen prior use or passed through columns of activated alumina and subsequently purged with nitrogen or argon. The starting materials 1-(di-phenylphosphino)imidazole,[1] $(t\text{-Bu})_2PBr$,[2] $[Au(tht)_2]OTf$[3], $[CuN(SiMe_3)_2]$[4] and $[AgN(SiMe_3)_2]$[5] were prepared according to the literature.

1.2 1-(di-tert-butylphosphino)imidazole

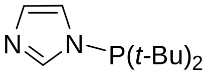

To a solution of imidazole (1.43 g, 21.04 mmol) and triethylamine (2.21 g, 21.80 mmol) in Et_2O (15 ml) was added a solution of di-*tert*-butylchlorophosphine (3.62 g, 20.04 mmol) in Et_2O (10 ml). After stirring overnight at room temperature, the precipitate was filtered off and washed twice with Et_2O. The combined solutions were evaporated to dryness under reduced pressure. The residue was extracted twice with pentane and the filtrate was evaporated to dryness giving **1** as a colourless powder (4.03 g, 95%). The characterization data agree with those reported by Hofmann for the same compound.[6]

1.3 1,3-bis(di-tert-butylphosphino)-imidazolium triflate (1a)

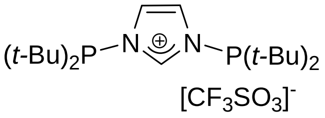

To a solution of 1-(di-tert-butylphosphino)imidazole (2.13 g, 10.03 mmol) and sodium triflate (2.01 g, 11.68 mmol) in THF (30 ml) was added dropwise at 0 °C pure di-*tert*-butylbromophosphine (2.59 g, 11.51 mmol). The reaction mixture was allowed to warm slowly to room temperature and was stirred for 24 h. The solvent was removed in vacuo, and the residue was extracted with CH_2Cl_2 (3×30 ml). The extracts were evaporated to dryness under reduced pressure, and the residue was washed with pentane (2×40 ml) to give **1a** as a colourless powder (4.30 g, 85%). X-ray quality crystals were obtained by slow diffusion of pentane into a THF solution of **1a**. Analysis: Found (Calc. for $C_{20}H_{39}F_3N_2O_3P_2S{\bullet}0.1CH_2Cl_2$) (%): C, 46.45 (46.87), H, 7.61 (7.67), N, 5.35 (5.44). ^1H NMR (400 MHz, $CDCl_3$): δ 8.43 (s, 1H, NC*H*N), 8.18 (s, 2H, im-*H*), 1.27 (d, 36H, $^3J_{HP}$ = 13.7 Hz, $C(CH_3)_3$). $^{13}C\{^1H\}$ NMR (125 MHz, $CDCl_3$): δ 146.9 (t, $^2J_{CP}$ = 31.6 Hz, N*C*HN), 129.1 (N*C*H=*C*HN), 121.0 (q, $^1J_{CF}$ = 319.8 Hz, CF_3), 35.5 (d, $^1J_{CP}$ = 29.4 Hz, $C(CH_3)_3$), 28.6 (d, $^2J_{CP}$ = 16.0 Hz, $C(CH_3)_3$). $^{31}P\{^1H\}$ NMR (161 MHz, $CDCl_3$): δ 120.3 (s).

1.4 1-(di-tert-butylphosphino)-3-(diphenylphosphino)-imidazolium triflate (1b)

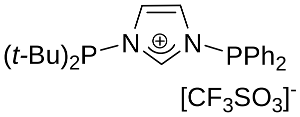

To a solution of 1-(di-phenylphosphino)imidazole (2.02 g, 8.01 mmol) and sodium triflate (1.70 g, 9.88 mmol) in THF (25 ml) was added dropwise at 0 °C pure di-tert-butylbromophosphine (2.10 g, 9.33 mmol). The reaction mixture was allowed to warm slowly to room temperature and stirred for 24 h. After removal of the solvent under reduced pressure, the residue was extracted with CH_2Cl_2 (3×25 ml). The extracts were evaporated to dryness and the solid residue was washed with Et_2O (2×30 ml) to give **2a** as a colourless powder (1.70 g, 39%). This imidazolium is very sensitive to air. Due to its sensitivity, a correct elemental analysis could not be obtained. ^{1}H NMR (400 MHz, $CDCl_3$): δ 8.41 (s, 1H, NC*H*N), 7.82 (s, 1H, im-*H*), 7.43-7.24 (m, 11H, im-*H* and Ar-*H*), 1.08 (d, 18H, $^3J_{HP}$ = 13.7 Hz, C(C*H*$_3$)$_3$). ^{13}C{^{1}H} NMR (75.5 MHz, $CDCl_3$): δ 145.4 (d, $^2J_{CP}$ = 33.8 Hz, N*C*HN), 132.9 (d, *J* = 23.3 Hz), 132.6, 131.3 (d, *J* = 15.4 Hz), 130.1 (d, *J* = 7.6 Hz), 129.0, 127, CF_3 carbon cannot be detected, 35.5 (d, $^1J_{CP}$ = 30.0 Hz, *C*(CH$_3$)$_3$), 28.6 (d, $^2J_{CP}$ = 16.6 Hz, C(*C*H$_3$)$_3$). ^{31}P{^{1}H} NMR (161 MHz, $CDCl_3$): δ 122.2 (s), 69.7 (s).

1.5 1,3-bis(di-tert-butylphosphino)-imidazole-2-ylidene (2a)

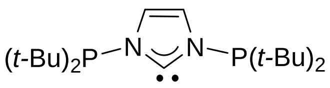

To a suspension of **1a** (2.00 g, 3.95 mmol) in ether (15 ml) at 0 °C was added dropwise a solution of sodium hexamethyldisilazide (0.76 g, 4.15 mmol) in ether (8 ml). The reaction mixture was allowed to warm to room temperature and stirred for 30 min. Evaporation of the solvent under reduced pressure, extraction of the residue into pentane (3×20 ml), evaporation of the extracts to dryness and washing of the solid residue with pentane (5 ml) at -40 °C gave **1b** as a colourless powder (0.70 g, 50%). X-ray quality crystals were obtained by slow cooling (-20 °C) of dilute pentane solutions for two days. ^{1}H NMR (400 MHz, C_6D_6): δ 6.93 (dd, 2H, $^3J_{HP}$ = 4.0 Hz, $^3J_{HH}$ = 1.6 Hz, im-*H*), 1.32 (d, 36H, $^3J_{HP}$ = 12.5 Hz, C(C*H*$_3$)$_3$). ^{13}C{^{1}H} NMR (125 MHz, C_6D_6): δ 232.7 (N*C*N), 126.5 (dd, $^2J_{CP}$ = 34.2 Hz, $^3J_{CP}$ = 7.0 Hz, NCH=*C*HN), 35.4 (d, $^1J_{CP}$ = 24.6 Hz, *C*(CH$_3$)$_3$), 29.6 (d, $^2J_{CP}$ = 16.1 Hz, C(*C*H$_3$)$_3$). ^{31}P{^{1}H} NMR (161 MHz, C_6D_6): δ 98.7 (s). Due to the sensitivity of **2a**, a correct elemental analysis could not be obtained.

1.6 1,2-bis(di-tert-butylphosphino)-1H-imidazole (3a)

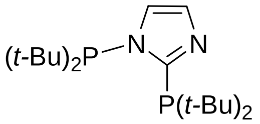

A Young's NMR tube charged with **2a** (*ca.*12 mg) and toluene-d^8 (0.4 ml) was heated to 120 °C overnight. In the ^{31}P{^{1}H} NMR the peak for **2a** at 98 ppm disappeared. ^{1}H NMR (400 MHz, toluene-d^8): δ 7.32 (s, 1H, im-*H*), 7.09-7.08 (2H, im-*H* and toluene), 1.37 (d, 18H, $^3J_{HP}$ = 11.7 Hz, C(C*H*$_3$)$_3$), 1.03 (d, 18H, $^3J_{HP}$ = 12.0 Hz, C(C*H*$_3$)$_3$). ^{13}C{^{1}H} NMR (125 MHz, toluene-d^8): δ 156.1 (dd, $^1J_{CP}$ = 24.8 Hz, $^2J_{CP}$ = 19.9 Hz, N*C*N), 131.3 (N*C*H=CHN), 124.3 (d, $^3J_{CP}$ = 7.0 Hz, NCH=*C*HN), 35.7 (d, $^1J_{CP}$ = 32.5 Hz, *C*(CH$_3$)$_3$), 34.6 (d, $^1J_{CP}$ = 20.7 Hz, *C*(CH$_3$)$_3$), 31.2 (d, $^2J_{CP}$ = 14.7 Hz, C(*C*H$_3$)$_3$), 29.8 (d, $^2J_{CP}$ = 17.2 Hz, C(*C*H$_3$)$_3$). ^{31}P{^{1}H} NMR (161 MHz, toluene-d^8): δ 78.2 (d, $^3J_{PP}$ = 90.0 Hz, (*t*-Bu)$_2$*P*-N), 7.9 (d, $^3J_{PP}$ = 90.0 Hz, (*t*-Bu)$_2$*P*-C).

1.7 1-(di-tert-butylphosphino)-2-(diphenylphosphino)-1H-imidazole (3b)

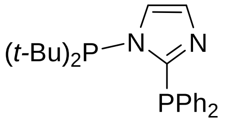

To a suspension of **1b** (0.52 g, 0.95 mmol) in Et_2O (8 ml) at 0 °C was added dropwise a solution of sodium hexamethyldisilazide (0.18 g, 1.00 mmol) in Et_2O

(5 ml). The reaction mixture was allowed to warm to room temperature and stirred for 30 min. Evaporation of the volatiles under reduced pressure, extraction of the residue with pentane (3×20 ml), evaporation of the extracts to dryness and washing of the remaining solid with pentane (5 ml) at -40 °C gave **3b** as a colourless powder (0.10 g, 27%). Analysis: Found (Calc. for $C_{23}H_{30}N_2P_2$) (%): C, 69.42 (69.68), H, 7.52 (7.63), N, 6.90 (7.07). ^{1}H NMR (400 MHz, CD_2Cl_2): δ 7.45 (dd, 1H, $^3J_{HP}$ = 2.1 Hz, $^3J_{HH}$ = 1.3 Hz, im-*H*), 7.43-7.38 (4H, Ar-*H*), 7.32-7.29 (6H, Ar-*H*), 7.26 (t, 1H, $^3J_{HH}$ = 1.2 Hz, im-*H*), 1.11 (d, 18H, $^3J_{HP}$ = 12.6 Hz, C(C*H*$_3$)$_3$). ^{13}C{^{1}H} NMR (125 MHz, CD_2Cl_2): δ 155.7 (d, $^1J_{CP}$ = 22.8 Hz, N*C*N), 137.0 (dd, *J* = 8.2 Hz, *J* = 5.3 Hz), 134.5(d, $^1J_{CP}$ = 21.0 Hz, Ar-*C*P), 132.2, 129.0, 128.5 (d, *J* = 7.3 Hz), 125.4 (d, *J* = 7.4 Hz), 35.6 (dd, $^1J_{CP}$ = 28.7 Hz, *J* = 2.1 Hz, *C*(CH$_3$)$_3$), 29.1 (d, $^2J_{CP}$ = 16.2 Hz, C(*C*H$_3$)$_3$). ^{31}P{^{1}H} NMR (161 MHz, CD_2Cl_2): δ 80.0 (d, $^3J_{PP}$ = 115.4 Hz, *P*(*t*-Bu)$_2$), -28.2 (d, $^3J_{PP}$ = 115.4 Hz, *P*Ph$_2$).

1.8 $[Cu_3\{\mu_3\text{-}\kappa^3 P,C,P\}_2](CF_3SO_3)_3$ (Cu-1)

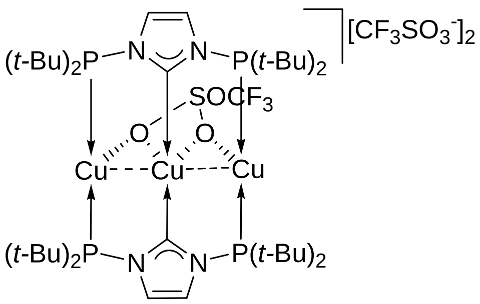

To a solution of $(CuO_3SCF_3)_2$•Toluene (0.11 g, 0.21 mmol) in THF (8 ml) was added a solution of **2a** (0.10 g, 0.28 mmol) in THF (5 ml) at -10 °C. The reaction mixture was allowed to warm slowly to room temperature and stirred for 3 h leading to the formation of a precipitate. After removal of the mother liquor by filtration, the solid was washed with ether (2×10 ml) and dried under vacuum to give **Cu-1** as a white powder (0.17 g, 90%). X-ray quality crystals were obtained by slow diffusion of ether into dichloromethane solution of **Cu-1**. Analysis: Found (Calc. for $C_{41}H_{76}Cu_3F_9N_4O_9P_4S_3$) (%): C, 35.96 (36.46), H, 5.76 (5.67), N, 3.83 (4.15). ^{1}H NMR (400 MHz, CD_2Cl_2): δ 8.09 (s, 4H, im-*H*), 1.51 (t, 72H, $^3J_{HP}$ = 8.4 Hz, C(C*H*$_3$)$_3$). ^{13}C{^{1}H} NMR (125 MHz, CD_2Cl_2): δ 194.2 (t, $^2J_{CP}$ = 22.4 Hz, N*C*N), 128.1 (N*C*H=*C*HN), 120.9 (q, $^1J_{CF}$ = 320.4 Hz, *C*F$_3$), 38.5 (*C*(CH$_3$)$_3$), 29.6 (C(*C*H$_3$)$_3$). ^{31}P{^{1}H} NMR (161 MHz, CD_2Cl_2): δ 102.1 (s).

1.9 $[Ag_3\{\mu_3\text{-}\kappa^3 P,C,P\}_2](CF_3SO_3)_3$ (Ag-1)

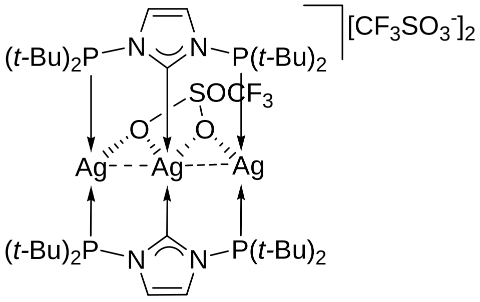

To a solution of AgO_3SCF_3 (0.13 g, 0.50 mmol) in THF (8 ml) was added a solution of **2a** (0.12 g, 0.33 mmol) in THF (5 ml) at -10 °C. The reaction mixture was allowed to warm slowly to room temperature and stirred for 3 h. A precipitate formed and after removing of the supernant, the solid was washed with Et_2O (2×10 ml) and dried under vacuum to give **Ag-1** as a white powder (0.22 g, 89%). X-ray quality crystals were obtained by slow diffusion of ether into dichloromethane solution of **Ag-1**. Analysis: Found (Calc. for $C_{41}H_{76}Ag_3F_9N_4O_9P_4S_3$•$CH_2Cl_2$) (%): C, 31.92 (32.16), H, 5.07 (5.01), N, 3.59 (3.57). ^{1}H NMR (400 MHz, CD_3CN): δ 7.97 (s, 4H, im-*H*), 1.45 (t, 72H, $^3J_{HP}$ = 8.2 Hz, C(CH_3)$_3$). $^{13}C\{^1H\}$ NMR (125 MHz, CD_3CN): δ 200.3 (overlapping m, $^1J_{C\text{-}109Ag}$ = 213.1 Hz, $^1J_{C\text{-}107Ag}$ = 184.2 Hz, N*C*N), 128.6 (N*C*H=*C*HN), 122.4 (q, $^1J_{CF}$ = 321.4 Hz, *C*F$_3$), 38.7(*C*(CH$_3$)$_3$), 29.3(C(*C*H$_3$)$_3$). $^{31}P\{^1H\}$ NMR(161 MHz, CD_3CN): two doublets at δ 119.4 ($J_{P\text{-}109Ag}$ = 541.0 Hz, $J_{P\text{-}107Ag}$ = 467.3 Hz).

1.10 [$Au_3\{\mu_3\text{-}\kappa^3 P,C,P\}_2$]($CF_3SO_3$)$_3$ (Au-1)

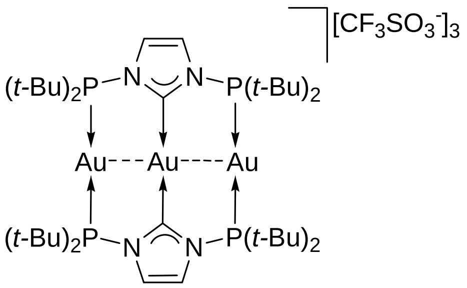

To a solution of [Au(tht)$_2$]O_3SCF_3 (0.091 g, 0.17 mmol) in THF (4 ml) was added a solution of **2a** (0.042 g, 0.12 mmol) in THF (6 ml) at -10 °C. The reaction mixture was allowed to warm slowly to room temperature and stirred for 3 h leading to the formation of a precipitate. After removal of the mother liquor by filtration, the solid was washed with dichloromethane (3 ml) and dried under vacuum to give **Au-1** as a white powder (0.056 g, 56%). X-ray quality crystals were obtained by slow diffusion of ether into acetonitrile solution of **Au-1**. Analysis: Found (Calc. for $C_{41}H_{76}Au_3F_9N_4O_9P_4S_3\bullet 0.5CH_3CN$) (%): C, 28.85 (28.47), H, 4.60 (4.41), N, 3.09 (3.56). ^{1}H NMR (400 MHz, CD_3CN): δ 8.17 (s, 4H, im-*H*), 1.57 (t, 72H, $^3J_{HP}$ = 9.5 Hz, C(CH_3)$_3$). $^{13}C\{^1H\}$ NMR (125 MHz, CD_3CN): δ 194.3 (t, $^2J_{CP}$ = 14.6 Hz, N*C*N), 129.8 (N*C*H=*C*HN), 122.2 (q, $^1J_{CF}$ = 321.7 Hz, *C*F$_3$), 41.5 (*C*(CH$_3$)$_3$), 29.5 (C(*C*H$_3$)$_3$). $^{31}P\{^1H\}$ NMR(161 MHz, CD_3CN): δ 141.0 (s).

1.11 [$Cu_2\{\mu_2\text{-}\kappa^2 C,P\}_2$]($CF_3SO_3$)$_2$ (Cu-2)

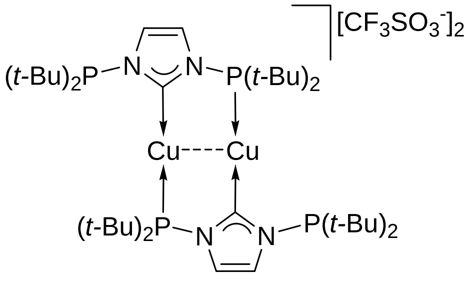

To a suspension of [CuN(SiMe$_3$)$_2$] (0.11 g, 0.50 mmol) in THF (7 ml) was added a solution of **1a** (0.25 g, 0.50 mmol) in THF (8 ml) at -10 °C. The reaction mixture was allowed to warm slowly to room temperature and stirred for 1 h resulting in the formation of a precipitate. After evaporation of the solvent under reduced pressure, the residue was washed with ether (10 ml) and dried under vacuum to give **Cu-2** as a white powder (0.25 g, 88%). X-ray quality crystals were obtained by slow diffusion of pentane into a THF solution of **Cu-2**. Analysis: Found (Calc. for $C_{40}H_{76}Cu_2F_6N_4O_6P_4S_2$) (%): C, 42.32 (42.21), H, 6.93 (6.73), N, 4.90 (4.92). ^{1}H NMR (400 MHz, THF-d^8): δ 7.86 (s, 4H, im-*H*), 1.40 (b, 72H, C(CH_3)$_3$). $^{13}C\{^1H\}$ NMR (125 MHz, THF-d^8): δ 201.5 (N*C*N), 126.6 (N*C*H=*C*HN), 122.1 (q, $^1J_{CF}$ = 323.2 Hz, *C*F$_3$), 36.1 (b, *C*(CH$_3$)$_3$), 29.6 (b, C(*C*H$_3$)$_3$). $^{31}P\{^1H\}$ NMR (161 MHz, THF-d^8): δ 94.5 (b).

1.12 [$Ag_2\{\mu_2\text{-}\kappa^2 C,P\}_2$]($CF_3SO_3$)$_2$ (Ag-2)

Method a: A solution of AgO_3SCF_3 (0.128 g, 0.50 mmol) and NaN(SiMe$_3$)$_2$ (0.092 g, 0.50 mmol) in toluene (8 ml) was stirred for 15 min at room temp. in the dark. A solution of **1a** (0.253 g, 0.50 mmol) in THF (8 ml) was added and stirred for another 20 min. After removal of the mother liquor by filtration, dissolution of the solid in CH_2Cl_2, filtration and evaporation of the filtrate to give a mixture of **Ag-1** and **Ag-2** as a white powder. ^{1}H NMR (400 MHz, CD_2Cl_2): δ 7.82 (s, 4H, im-*H*), 1.36 (d, 72H, $^3J_{HP}$ = 14.5 Hz, C(CH_3)$_3$). ^{13}C{^{1}H} NMR (125 MHz, CD_2Cl_2): δ 203.5 (overlapping m, N*C*N), 127.0 (NCH=*C*HN), 120.9 (q, $^1J_{CF}$ = 322.1 Hz, *C*F_3), 36.4 (b, *C*(CH_3)$_3$), 28.8 (b, C(*C*H_3)$_3$). ^{31}P{^{1}H} NMR (161 MHz, CD_2Cl_2): two broad mutiplets at δ 116.7.

Method b: To a suspension of Ag_2O (0.136 g, 0.27 mmol) with molecular sieves 4 Å (ca. 0.4 g) in CH_2Cl_2 (10 ml) was added a solution of **1a** (0.062 g, 0.27 mmol) in CH_2Cl_2 (10 ml). The reaction mixture was stirred for 3 days at room temperature. After filtering off the solid, the filtrate was evaporated to dryness under reduced pressure to give **Ag-2** as a white powder.

2. X-ray crystallography

Summary of the crystal data, data collection and refinement for structures of **1a**, **2a**, **Cu-1**• $2CH_2Cl_2$, **Ag-1**• $2CH_2Cl_2$, **Au-1**• 2MeCN and **Cu-2** are given in Table S1. The crystals were mounted on a glass fiber with grease, from Fomblin vacuum oil. Data sets were collected on a Bruker APEX II DUO diffractometer equipped with an Oxford Cryosystem liquid N_2 device, using Mo-Kα radiation (λ = 0.71073 Å). The crystal-detector distance was 38 mm. The cell parameters were determined (APEX2 software)[7] from reflections taken from three sets of 12 frames, each at 10 s exposure. The structures were solved by direct methods using the program SHELXS-97.[8] The refinement and all further calculations were carried out using SHELXL- 97.[9] The H-atoms were included in calculated positions and treated as riding atoms using SHELXL default parameters. The non-H atoms were refined anisotropically, using weighted full-matrix least-squares on F^2.

The following special comments apply to the models of the structures:

For **1a**, the methyls groups C9, C10, C11 are disordered on two positions. A squeeze procedure was applied and the residual electron density was assigned to half a molecule of THF.

The asymmetric unit of **Cu-1**• $2CH_2Cl_2$ contains half a molecule of the copper complex, three half molecules of triflate and two half molecules of dichloromethane. The atoms C1, C11, C21, C22, C23, C24, C25, O2, O3, O6, F2, F3, F6, S1, S2, S3, Cu1, Cl1, Cl2, Cl3 and Cl4 are in special position (population 50%). The methyls : C8, C9 and C10 are disordered on two positions.

In the structure of **Ag-1**• $2CH_2Cl_2$, the asymmetric unit contains half a molecule of this complex, three half molecules of triflates and two half molecules of dichloromethane. The atoms : C1, C11, C21, C22, C23, C24, C25, O2, O4, O6, F2, F4, F6, S1, S2, S3, Ag1, Cl1, Cl2, Cl3 and Cl4 are in special position (population 50%). The methyls : C18, C19 and C20 are disordered on two positions.

The asymmetric unit of **Au-1**• 2MeCN contains two half molecules of the cation, 3 molecules of triflate and 2 molecules of MeCN. One triflate anion is disordered over two positions.

2.1 Summary of crystal data

Table S1. Crystal data for compounds **1a**, **2a**, **Cu-1**• $2CH_2Cl_2$, **Ag-1**• $2CH_2Cl_2$, **Au-1**• 2MeCN and **Cu-2**.

	1a	**2a**	**Cu-1**• $2CH_2Cl_2$	**Ag-1**• $2CH_2Cl_2$	**Au-1**• 2MeCN	**Cu-2**
Chemical formula	$C_{20}H_{39}F_3N_2O_3P_2S$	$C_{19}H_{38}N_2P_2$	$C_{41}H_{76}Cu_3F_9N_4O_9P_4S_3 \cdot 2CH_2Cl_2$	$C_{41}H_{76}Ag_3F_9N_4O_9P_4S_3 \cdot 2CH_2Cl_2$	$C_{41}H_{76}Au_3F_9N_4O_9P_4S_3 \cdot 2CH_3CN$	$C_{40}H_{76}Cu_2F_6N_4O_6P_4S_2$
CCDC Number	963084	963085	963087	963088	963089	963086
Formula Mass	506.53	356.45	1520.59	1653.58	1833.13	1138.13
Crystal system	Monoclinic	Monoclinic	Orthorhombic	Orthorhombic	Triclinic	Monoclinic
a/Å	11.9434(18)	23.8815(12)	16.4659(12)	16.5334(6)	12.0469(6)	8.8473(5)
b/Å	11.9397(18)	12.4951(6)	15.6201(13)	15.6264(5)	12.6938(6)	13.1451(7)
c/Å	20.730(3)	15.9372(8)	24.952(2)	25.5667(7)	24.4780(12)	23.5989(13)
α/°	90	90	90	90	90.0060(10)	90
β/°	93.356(3)	108.7810(10)	90	90	103.5620(10)	94.3950(10)
γ/°	90	90	90	90	116.8880(10)	90
Unit cell volume/Å^3	2951.1(8)	4502.5(4)	6417.7(9)	6605.3(4)	3221.0(3)	2736.4(3)
Temperature/K	173(2)	173(2)	173(2)	173(2)	173(2)	173(2)
Space group	*P21/c*	*C2/c*	*Pnma*	*Pnma*	*P-1*	*P21/c*
Formula units / cell, Z	4	8	4	4	2	2
Absorption coefficient, μ/mm^{-1}	0.257	0.196	1.425	1.308	7.09	1.034
No. of reflections measured	20827	48197	25849	34171	59662	22020
No. of independent reflections	7188	6585	8034	10868	20683	7272
R_{int}	0.0703	0.0294	0.102	0.0382	0.0313	0.0486
Final R_1 values ($I > 2\sigma(I)$)	0.0806	0.0436	0.0741	0.0454	0.0372	0.0742
Final $wR(F^2)$ values ($I > 2\sigma(I)$)	0.1835	0.1054	0.1619	0.0904	0.0713	0.2009
Final R_1 values (all data)	0.1344	0.0581	0.1819	0.0973	0.0593	0.119
Final $wR(F^2)$ values (all data)	0.2026	0.116	0.216	0.1137	0.0782	0.2284
Goodness of fit on F^2	1.018	1.107	1.022	1.048	1.064	1.038

2.2 The crystal structure of 1a

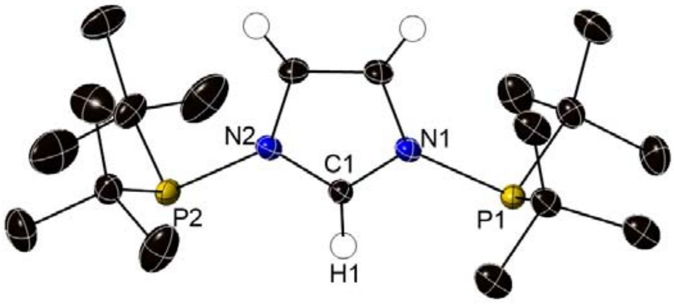

Figure S1. Thermal ellipsoid representation (30% probability level) of the structures of **1a**. One triflate anion and H atoms except those attached to the heterocyclic ring are omitted for clarity; only one disordered position of one ^{t}Bu at P1 is shown. Selected bond lengths (Å) and angles [°]: C1-N1 1.320(4); C1-N2 1.331(4); C1-H1 0.9500; N1-P1 1.795(3); N2-P2 1.784(3); N1-C1-N2 110.9(3); N1-C1-H1 124.6; N2-C1-H1 124.6; C1-N1-P1 119.6(2); C1-N2-P2 119.8(2).

2.3 The crystal structure of 2a

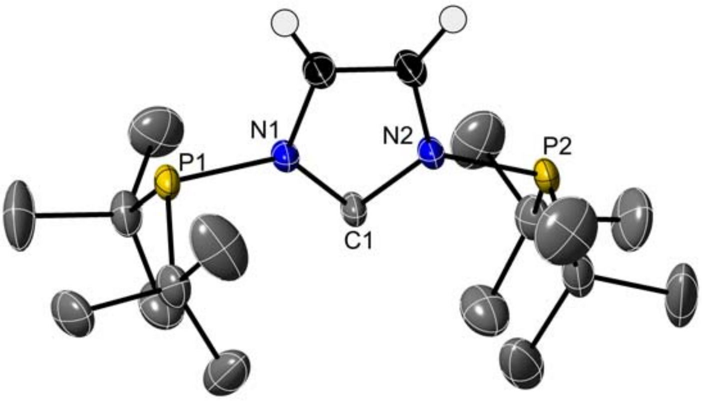

Figure S2. Thermal ellipsoid representation (30% probability level) of the structures of **2a**. H atoms except those attached to the heterocyclic ring are omitted for clarity. Selected bond lengths (Å) and angles [°]: C1-N1 1.3763(15); C1-N2 1.3779(14); N1-P1 1.7475(10); N2-P2 1.7531(11); N1-C1-N2 102.54(10); C1-N1-P1 128.91(8); C1-N2-P2 128.77(9).

2.4 The crystal structure of Ag-1• 2CH_2Cl_2

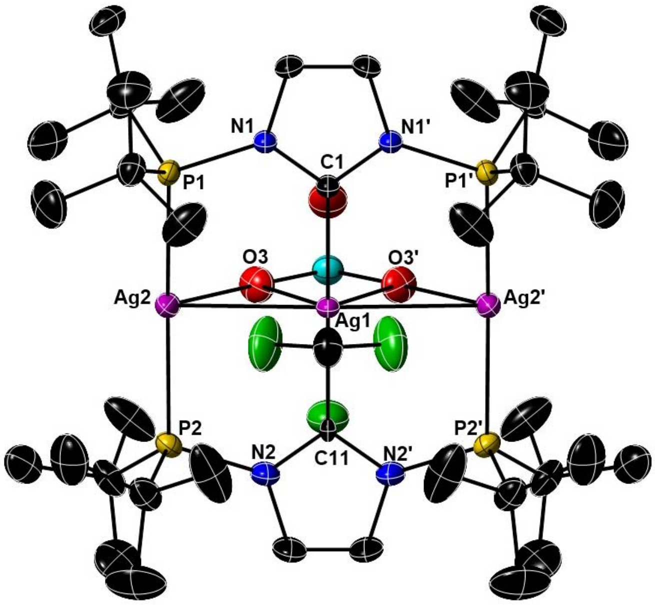

Figure S3. Thermal ellipsoid representation (30% probability level) of the cation in the structure of **Ag-1**•2CH_2Cl_2. Hydrogen atoms, uncoordinated triflate anions, disordered atoms and two molecules of solvent of crystallisation (CH_2Cl_2) are omitted for clarity. Selected bond lengths (Å) and angles [°]: C1-N1 1.337(4); C1-Ag1 2.152(4); C11-N2 1.332(4); C11-Ag1 2.161(4); N1-P1 1.745(3); N2-P2 1.754(3); P1-Ag2 2.4076(9); P2-Ag2 2.4046(9); Ag1-Ag2 2.7599(3); O3-Ag2 2.896; O3-Ag1 2.929; N1-C1-N1' 107.6(4); N1-C1-Ag1 126.19(19); N2-C11-N2' 108.4(4); N2-C11-Ag1 125.8(2); C1-N1-P1 125.2(2); C11-N2-P2 125.4(2); N1-P1-Ag2 109.12(9); C1-Ag1-C11 178.4(2); C1-Ag1-Ag2 90.368(14); C11-Ag1-Ag2 89.754(14); Ag2-Ag1-Ag2' 171.41(2); P2-Ag2-P1 164.93(4); P2-Ag2-Ag1 89.12(3); P1-Ag2-Ag1 88.85(2); Ag2-O3-Ag1 56.56; O3-Ag1-O3' 49.20.

References for the experimental part

1. S. Fischer, L. K. Peterson and J. F. Nixon, *Can. J. Chem.*, 1974, **52**, 3981-3985.
2. S. Humbel, C. Bertrand, C. Darcel, C. Bauduin and S. Juge, *Inorg. Chem.*, 2003, **42**, 420-427.
3. R. Usón, A. Laguna, A. Navarro, R. V. Parish and L. S. Moore, *Inorg. Chim. Acta.*, 1986, **112**, 205-208.
4. A. M. James, R. K. Laxman, F. R. Fronczek and A. W. Maverick, *Inorg. Chem.*, 1998, **37**, 3785-3791.
5. Y. Yamashita, T. Imaizumi, X.-X. Guo and S. Kobayashi, *Chem. –Asian J.*, 2011, **6**, 2550-2559.
6. P. Nägele, U. Herrlich, F. Rominger and P. Hofmann, *Organometallics*, 2012, **32**, 181-191.
7. Bruker AXS Inc Madison USA, 2006.
8. G. M. Sheldrick, *Acta Crystallogr. Sect. A: Found. Crystallogr.*, 1990, **A46**, 467.
9. G. M. Sheldrick, Universität Göttingen: Göttingen Germany, 1999.

3. Computational details

3.1 Methods and theory

Density functional theory (DFT) calculations were carried out using the Amsterdam Density Functional (ADF) program.[1,2] The numerical integration was performed using the procedure developed by te Velde et al.[2g,h] The molecular orbitals were expanded in a large set of uncontracted Slater-type orbitals (STOs) of triple-ζ quality augmented with two sets of polarisation functions for all atoms (TZ2P basis set),[2i] i.e. 2p and 3d on H, 3d and 4f on C, N, and P. An auxiliary set of s, p, d, f and g STOs was used to fit the molecular density and to represent the Coulomb and exchange potentials accurately in each self-consistent field cycle.[2j] All the structures herein analysed were optimised without any symmetry restrictions in the gas phase at the BP86 level since BP86 has been shown to be one of the three best generalised gradient approximation (GGA) DFT functionals (along with PBE and PW91) for geometry optimisations with the ADF program package.[3] The electronic exchange was described by Slater's Xα potential[2l] with self-consistent nonlocal corrections of Becke,[2m,n] and the electron correlation was treated in the Vosko-Wilk-Nusair (VWN) parameterisation[2o] with self-consistent nonlocal corrections of Perdew[2p] (BP86).[2q] The gas-phase energy minima were verified to be equilibrium structures through vibrational analyses with detailed surface scans.[4] The electron density distribution was analysed using the Hirshfeld scheme for computing atomic charges.[5] The energy decomposition analysis of the $N(\mathit{C}\text{-}\mathit{P}R_2)$ and N_{imid}–PR_2 bonds in the corresponding molecules was performed.[6]

3.2 Structural and energy analysis

Table S2. Energy costs associated with the different *syn*, *anti*-conformations of imidazolium cation in **1a**: relative energies (ΔE_{rel}, including zero-point energy corrections) and HOMO–LUMO gaps ($\Delta E_{H\text{–}L}$) are given. Colour code: H, off-white; C, grey; N, blue; P, orange.

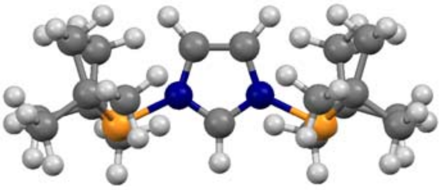	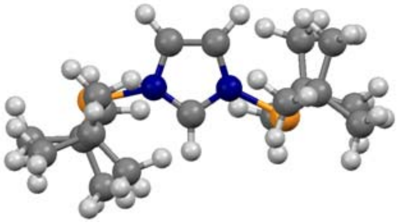	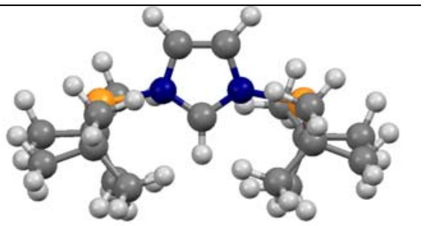
1a$_{\mathbf{comput}}$		
$E_{rel} = 0$ kJ·mol^{-1}	$E_{rel} = +3$ kJ·mol^{-1}	$E_{rel} = +9$ kJ·mol^{-1}
$\Delta E_{H\text{–}L} = 3.83$ eV	$\Delta E_{H\text{–}L} = 3.73$ eV	$\Delta E_{H\text{–}L} = 3.61$ eV

Table S3. Energy costs associated with the formation of N(*C*-PR$_2$) and N$_{\text{imid}}$–PR$_2$ bonds in the optimised structures and their *syn*, *anti*-conformers: relative energies (ΔE_{rel}, including zero-point energy corrections) and HOMO–LUMO gaps ($\Delta E_{\text{H–L}}$) are given. Hydrogen atoms are not shown for clarity. Colour code: H, off-white; C, grey; N, blue; P, orange.

syn, *anti*-conformers of N(*C*-*P*R$_2$) with R = *t*-Bu (top) and N(*C*-*P*R$_2$) with R = Ph (bottom)			*syn*, *anti*-conformers of N$_{\text{imid}}$–PR$_2$ with R = *t*-Bu (top) and N$_{\text{imid}}$–PR$_2$ with R = Ph (bottom)		
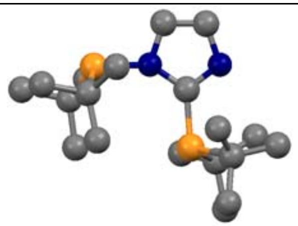	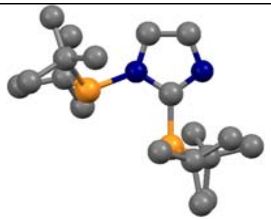	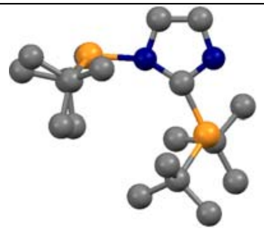	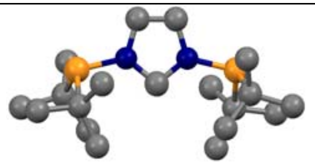	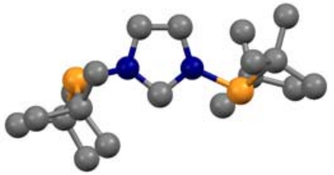	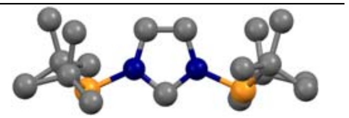
	3a$_{\mathbf{comput}}$		**2a**$_{\mathbf{comput}}$		
$\Delta E_{\text{rel}} = +30\ \text{kJ·mol}^{-1}$ $\Delta E_{\text{H–L}} = 3.99\ \text{eV}$	$\Delta E_{\text{rel}} = 0\ \text{kJ·mol}^{-1}$ $\Delta E_{\text{H–L}} = 3.75\ \text{eV}$	$\Delta E_{\text{rel}} = +134\ \text{kJ·mol}^{-1}$ $\Delta E_{\text{H–L}} = 3.57\ \text{eV}$	$\Delta E_{\text{rel}} = +89\ \text{kJ·mol}^{-1}$ $\Delta E_{\text{H–L}} = 4.05\ \text{eV}$	$\Delta E_{\text{rel}} = +99\ \text{kJ·mol}^{-1}$ $\Delta E_{\text{H–L}} = 4.10\ \text{eV}$	$\Delta E_{\text{rel}} = +115\ \text{kJ·mol}^{-1}$ $\Delta E_{\text{H–L}} = 4.02\ \text{eV}$
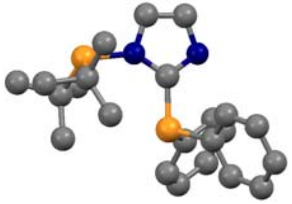	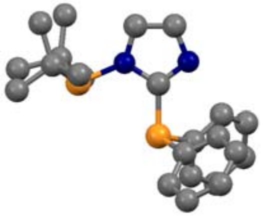	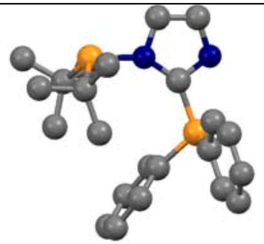	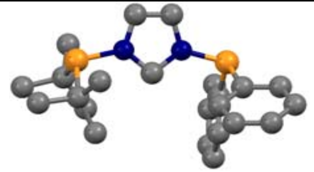	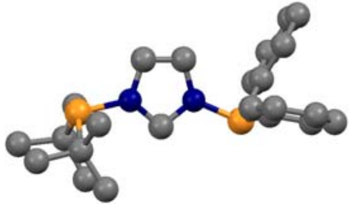	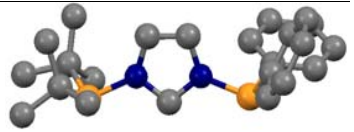
	3b$_{\mathbf{comput}}$				
$\Delta E_{\text{rel}} = +17\ \text{kJ·mol}^{-1}$ $\Delta E_{\text{H–L}} = 3.56\ \text{eV}$	$\Delta E_{\text{rel}} = 0\ \text{kJ·mol}^{-1}$ $\Delta E_{\text{H–L}} = 3.53\ \text{eV}$	$\Delta E_{\text{rel}} = +76\ \text{kJ·mol}^{-1}$ $\Delta E_{\text{H–L}} = 3.17\ \text{eV}$	$\Delta E_{\text{rel}} = +101\ \text{kJ·mol}^{-1}$ $\Delta E_{\text{H–L}} = 2.89\ \text{eV}$	$\Delta E_{\text{rel}} = +100\ \text{kJ·mol}^{-1}$ $\Delta E_{\text{H–L}} = 2.87\ \text{eV}$	$\Delta E_{\text{rel}} = +115\ \text{kJ·mol}^{-1}$ $\Delta E_{\text{H–L}} = 2.80\ \text{eV}$

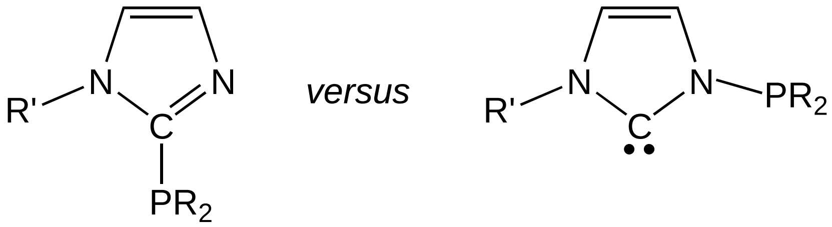

N(C-PR$_2$) isomer

N$_{imid}$-PR$_2$ isomer

	ΔD_e		ΔE_{H-L}			$\Delta\Delta E_{H-L}$	
	N(C-PR$_2$)	N$_{imid}$-PR$_2$	N(C-PR$_2$)		N$_{imid}$-PR$_2$	N(C-PR$_2$)	N$_{imid}$-PR$_2$
R' = Me							
R = *t*-Bu	0	-109	4.28	<	4.40	0	+0.12
Ph	0	-110	4.02	>	3.24	+0.78	0
R' = P*t*-Bu$_2$							
R = *t*-Bu	0	-89	3.75	<	4.05	0	+0.30
Ph	0	-100	3.53	>	2.87	+0.66	0
	kJ/mol		eV			eV	

Scheme S1. Energy costs associated with the formation of N(C-PR$_2$) and N$_{imid}$–PR$_2$ bonds in the optimized 'C–P' and 'N–P' isomers bearing different R' = Me, P*t*-Bu$_2$ and R = *t*-Bu, Ph substituents: relative bond dissociation energies (ΔD_e, in kJ·mol^{-1}) of N(C-PR$_2$) and N$_{imid}$–PR$_2$ bonds and HOMO–LUMO gaps (ΔE_{H-L}, in eV) are shown.

Hirshfeld charge analysis. The following evolution of the Hirshfeld atomic charges on phosphorous in the phosphenium R$_2$P$^+$ ions was found by DFT calculations: R = Ph (+0.32) < *t*-Bu (+0.36) < Me (+0.57) < H (+0.82). It is consistent with the fluoride ion affinity (FIA) scale obtained for the R$_2$P$^+$ cations by Slattery and Hussein.[7] The general trend in FIA was determined as follows: R = NR$_2$ < mesityl < SR < Ph < *t*-Bu < OR < C$_6$F$_5$ < I < Me < Br < Cl < F < H (increasing Lewis acidity).

References for the computational part

1. **ADF2010.01**, SCM, Theoretical Chemistry, Vrije Universiteit, Amsterdam, The Netherlands, http://www.scm.com. E. J. Baerends, J. Autschbach, A. Bérces, C. Bo, P. M. Boerrigter, L. Cavallo, D. P. Chong, L.Deng, R. M. Dickson, D. E. Ellis, L. Fan, T. H. Fischer, C. Fonseca Guerra, S. J. A. van Gisbergen, J. A. Groeneveld, O. V. Gritsenko, M. Grüning, F. E. Harris, P. van den Hoek, H. Jacobsen, G. van Kessel, F. Kootstra, E. van Lenthe, D. A. McCormack, V. P. Osinga, S. Patchkovskii, P. H. T. Philipsen, D. Post, C. C. Pye, W. Ravenek, P. Ros, P. R. T. Schipper, G. Schreckenbach, J. G. Snijders, M. Solà, M. Swart, D. Swerhone, G. te Velde, P. Vernooijs, L. Versluis, O. Visser, E. van Wezenbeek, G. Wiesenekker, S. K. Wolff, T. K. Woo and T. Ziegler.
2. (a) G. te Velde, F. M. Bickelhaupt, E. J. Baerends, C. Fonseca Guerra, S. J. A. van Gisbergen, J. G. Snijders and T. Ziegler, *J. Comput. Chem.*, 2001, **22**, 931; (b) C. Fonseca Guerra, O. Visser, J. G. Snijders, G. te Velde and E. J. Baerends, In *Methods and Techniques for Computational Chemistry*, (Eds.: E. Clementi, G. Corongiu), STEF: Cagliari, 1995, 305–395; (c) E. J. Baerends, D. E. Ellis and P. Ros, *Chem. Phys.*, 1973, **2**, 41; (d) E. J. Baerends and P. Ros, *Chem. Phys.*, 1975, **8**, 412; (e) E. J. Baerends and P. Ros, *Int. J. Quantum Chem. Symp.*, 1978, **12**, 169; (f) C. Fonseca Guerra, J. G. Snijders, G. te Velde and E. J. Baerends, *Theor. Chem. Acc.*, 1998, **99**, 391; (g) P. M. Boerrigter, G. te Velde and E. J. Baerends, *Int. J. Quantum Chem.*, 1988, **33**, 87; (h) G. te Velde and E. J. Baerends, *J. Comp. Phys.*, 1992, **99**, 84; (i) J. G. Snijders, P. Vernooijs and E. J. Baerends, *At. Nucl. Data Tables*, 1981, **26**, 483; (j) J. Krijn and E. J. Baerends, *Fit-Functions in the HFS-Method; Internal Report (in Dutch)*, Vrije Universiteit, Amsterdam, 1984; (k) L. Versluis and T. Ziegler, *J. Chem. Phys.*, 1988, **88**, 322; (l) J. C. Slater, *Quantum Theory of Molecules and Solids, Vol. 4*, McGraw-Hill, New York, 1974; (m) A. D. Becke, *J. Chem. Phys.*, 1986, **84**, 4524; (n) A. D. Becke, *Phys. Rev. A*, 1988, **38**, 3098; (o) S. H. Vosko, L. Wilk and M. Nusair, *Can. J. Phys.*, 1980, **58**, 1200; (p) J. P. Perdew, *Phys. Rev. B*, 1986, **33**, 8822 (Erratum: *Phys. Rev. B*, 1986, **34**, 7406); (q) L. Fan and T. Ziegler, *J. Chem. Phys.*, 1991, **94**, 6057.
3. M. Swart and J. G. Snijders, *Theor. Chem. Acc.*, 2003, **110**, 34. Erratum: *Theor. Chem. Acc.*, 2004, **111**, 56.
4. (a) A. Bérces, R. M. Dickson, L. Fan, H. Jacobsen, D. Swerhone and T. Ziegler, *Comput. Phys. Commun.*, 1997, **100**, 247; (b) H. Jacobsen, A. Bérces, D. Swerhone and T. Ziegler, *Comput. Phys. Commun.*, 1997, **100**, 263; (c) S. K. Wolff, *Int. J. Quantum Chem.*, 2005, **104**, 645.
5. F. L. Hirshfeld, *Theor. Chim. Acta*, 1977, **44**, 129.
6. (a) A. Krapp, F. M. Bickelhaupt and G. Frenking, *Chem. Eur. J.*, 2006, **12**, 9196; (b) F. M. Bickelhaupt and E. J. Baerends, In *Reviews in Computational Chemistry*; Lipkowitz K. B.; Boyd D. B. Eds.; Wiley-VCH: New York, 2000; **15**, 1; (c) F. M. Bickelhaupt, A. Diefenbach, S. P. de Visser, L. J. de Koning and N. M. M. Nibbering, *J. Phys. Chem. A*, 1998, **102**, 9549; (d) F. M. Bickelhaupt, N. M. M. Nibbering, E. M. van Wezenbeek and E. J. Baerends, *J. Phys. Chem.*, 1992, **96**, 4864; (e) T. Ziegler and A. Rauk, *Inorg. Chem.*, 1979, **18**, 1558; (f) T. Ziegler and A. Rauk, *Inorg. Chem.*, 1979,

18, 1755; (g) T. Ziegler and A. Rauk, *Theor. Chim. Acta*, 1977, **46**, 1; (h) K. Morokuma, *Acc. Chem. Res.*, 1977, **10**, 294; (i) K. Kitaura and K. Morokuma, *Int. J. Quantum Chem.*, 1976, **10**, 325.

7. J. M. Slattery, S. Hussein, *Dalton Trans.*, 2012, **41**, 1808.